

Full Length Research Paper

Effects of the incorporation of carbon spheres into nanostructured TiO₂ film for dye-sensitized solar cell

Shishu Fu, Feitao Li, Zhuoyu Huo and Yuzong Gu*

Institute of Microsystem Physics, Henan University, Kaifeng 475004, China.

Accepted 24 March, 2011

Nanoporous TiO₂ thin film electrodes were fabricated based on incorporating various amounts of carbon spheres into TiO₂ paste followed by thermal treatment. The size of carbon spheres was prepared from 100 to 200 nm. The TiO₂ electrodes modified with carbon spheres were characterized by X-ray diffraction, scanning electron microscopy, X-ray photoelectron spectroscopy and UV-visible spectrophotometer. The performances of dye-sensitized solar cells with carbon-sphere-modified TiO₂ anodes were investigated. The experimental results indicated that 1.0 wt% of carbon spheres with the size of 100 nm added into TiO₂ anode had the most favorable effect on the performance of dye-sensitized solar cells compared with other quantities and sizes. The incipient performance of the dye-sensitized solar cell in the investigation was: a V_{oc} of 0.71 V, a J_{sc} of 12.00 mA cm⁻², a fill factor of 56.92% and an efficiency of 4.85%, which was enhanced comparing with that of carbon-free TiO₂ electrode under the same experimental conditions. The results revealed the possibility of fabricating dye-sensitized solar cells using nanometer-sized carbon spheres.

Key words: Carbon spheres, TiO₂ films, dye-sensitized solar cell.

INTRODUCTION

Dye-sensitized solar cells (DSSCs) have been extensively studied due to their high photoelectric conversion efficiency, simple assemble technology, and potential low cost for 30 years (O'Regan et al., 1991; Grätzel, 2007). The improvement in efficiency of DSSCs is due to larger surface area of porous film, more efficient light absorption of dye molecules, and faster electron transport and/or transfer between the interfaces of film material/electrolyte/counter electrode within DSSCs (Tan et al., 2006; Zhao et al., 2008). For a DSSC employing TiO₂ film as anode, photoelectric conversion efficiency of DSSCs is affected by many factors, such as counter electrode (Fang et al., 2004), transmittance and conductivity of conducting glass (Podraza et al., 2005), electrolyte composition (Hara et al., 2005), type of dye sensitizer (Nazeeruddin et al., 2001), and structures of TiO₂ film (Wang et al., 2004; Nakade et al., 2003; Saito et al., 2004; Grätzel, 2004). Particularly, the crystallite size, porous structure and morphology of TiO₂ film electrode play important roles in the photoelectric conversion

efficiency of DSSCs (Tan et al., 2006; Mor et al., 2006; Zhao et al., 2008). The surface area is controlled by the size of particles and the thickness of films. Therefore, various approaches up to date have been tried to optimize these parameters by means of fabricating nanocrystalline and nanoporous metal oxide films.

Chou et al. (2007) reported the titania particle size effect on the performance of DSSCs. Nakade et al. (2003) demonstrated that the diffusion coefficients of electrons in the TiO₂ film increase but the recombination lifetime decreases with particle size. Ni et al. (2006) researched that the optimal porosity in a DSSC can affect light absorption and electron diffusion. The Frank group (Benkstein et al., 2003) confirmed that the porosity increased greatly with the amount of polyethylene glycol (PEG). But the optimum porosity of nanostructured TiO₂ film fabricated for DSSCs was about 50–65% (Lagemaat et al., 2001). Shen et al. (2003) reported optical absorption and electron transport properties of TiO₂ film with different pore sizes and proposed that small TiO₂ particles and large pore size can get good electron transport and high conversion efficiency. Moreover, Lee et al. (2009) observed that morphology of TiO₂ film strongly influences the performance of the DSSC. So far,

*Corresponding author. E-mail: guyuzong@yahoo.com.cn. Tel: +86 378 3881602. Fax: +86 378 3881602.

various morphological TiO₂ porous photoanodes have been fabricated to increase the surface area of nanoporous TiO₂ film such as nanoparticles (Grätzel, 2004; Zhao et al., 2008), nanowires (Tao et al., 2010), nanofibers (Song et al., 2004), titanium threads and titanium sheet (Wang et al., 2009) and nanotubes (Chou et al., 2007). Yu et al. (2010) reported that calcination temperatures exhibit a strong influence on the microstructure and photoelectric conversion efficiency of HA-TiO₂ DSSCs. It has been known that the higher the surface area of TiO₂, the higher the current is generated by the DSSC (Park et al., 2000).

In this paper, we only studied the effects of carbon spheres after the introduction of the TiO₂ paste on the performance of DSSC without considering other impacting parameters. Carbon spheres were prepared by glucose aqueous solution which gave rise to smooth surface and stable mechanical properties. Carbon spheres have some advantages, such as low cost due to the inexpensive glucose aqueous solution, and the fact that various sizes and structures can be readily available under different controlling conditions. The formation of porous and nanoparticulated TiO₂ films were presented using carbon spheres with two different diameters (100 and 200 nm). The incorporation of carbon spheres into the TiO₂ paste would theoretically influence the surface area and the average size of the particle of TiO₂ electrodes due to the reactions between the carbon spheres and oxygen from the TiO₂ lattices and the air atmosphere to form CO₂ gas in the high-temperature sintering process. The effects of carbon spheres added with different amounts and sizes were experimentally studied.

MATERIALS AND METHODS

TiO₂ powder (P-25) was purchased from Degussa AG. All chemicals were reagent grade. An optically transparent conducting glass (FTO, sheet resistance 8 Ω sq⁻¹, transmittance 77% in the visible range) was used as a substrate. The substrate was cleaned in acetone, ethanol and DI water for 20 min in turns.

Carbon spheres with diameters of 100 and 200 nm were prepared by hydrothermal treatment of 0.5 M glucose aqueous solution in a teflon-lined autoclave at 170°C for 3 and 4.5 h respectively, according to the report of Sun et al. (2004).

Nanocrystalline TiO₂ powder (P25, Degussa, 0.6 g) and carbon spheres with the diameters of 100 or 200 nm (from 0 to 3 wt% versus TiO₂ weight) were ground together for a while and then acetylacetone, polyethylene glycol (PEO, M_v = 100,000; 20 wt% versus TiO₂ weight), and DI water were added. The nanoporous TiO₂ films were made onto a conducting glass from the prepared paste using scotch tape as frame and spacer by the doctor blade technique, dried for 5 min using a dryer, sintered at 450 °C for 1 h and then heated again at 550°C for 30 min (the TiO₂ film containing 1 wt% carbon spheres) or 50 min (the TiO₂ film containing 2, 3 wt% carbon spheres) in the air. The thermal treatment used in the second-step must be conducted, in order to completely remove the incorporated carbon elements through their chemical reaction (Kang et al., 2007a). The TiO₂ electrode used as the control sample without any incorporation of carbon spheres was fabricated by the addition of polyethylene glycol (Mn: 8000, 20 wt% versus TiO₂

weight, conventional porosity induced material) to the TiO₂ paste and played the role of a standard.

Having been heated (80 ~ 90 °C) for 10 min, the TiO₂ film was dipped in a 0.5 mM ethanol solution of N719 for 24 h to absorb the dye adequately. Subsequently, the other impurities on the TiO₂ anodes were rinsed with the anhydrous ethanol and the TiO₂ anodes were dried in the air at 70 °C for 10 min to remove the adsorbed moisture and redundant organics before electrochemical experiment. Then, the TiO₂ electrode and the Pt counter electrode were fastened by two clips. Following that, a drop of the redox electrolyte was introduced into the cell by capillary action which composed of 0.5 M Lil, 0.05 M I₂, and 0.5 M 4-tert-butylpyridine in acetonitrile solution. After that, a dye-sensitized TiO₂ cell was obtained.

Transmission electron microscopy (TEM, JEM-100cx, JEOL) was applied to examine the morphology of the carbon sphere and scanning electron microscopy (SEM, JSM-5600LV, JEOL) was used to characterize the morphology of the TiO₂ electrodes. X-ray diffraction (XRD, DX-2500, Fangyuan) measurement was performed on a diffractometer with Cu Kα radiation with λ=1.54145 Å and all samples were scanned from 20 to 80° at a rate of 0.02 scans/second to determine the phase structures of the obtained samples and their crystallite size.

The surface area values found from BET were very similar to that found from theoretical calculation with a difference of ~0.2 m² g⁻¹ (Chou et al., 2007). Therefore, the theoretical values of the surface area were estimated using the crystal size results from X-ray diffraction (XRD) analysis. The theoretical value of the surface area is calculated using the following equations:

$$SA = \frac{\#_{particles} \cdot A_{particle}}{W_{sample}} \quad (1)$$

$$\#_{particles} = \frac{V_{sample}}{V_{particle}} = \pi R^2 h / \left(\frac{4}{3} \right) \pi r^3 \quad (2)$$

$$A_{particle} = 4\pi r \cdot 10^{-4} \quad (3)$$

where SA is surface area (m² g⁻¹), #_{particles} is number of particles, A_{particle} is area of each particle (m²), W_{sample} is total sample weight (g), V_{sample} is volume of sample area (cm³), V_{particle} is volume of each spherical particle (cm³), R is radius of sample area (cm), h is thickness of film sample (cm), r is radius of each particle (cm).

In addition, X-ray photoelectron spectroscopy (XPS) (PHI 5200 mode) was performed to investigate the existence of remaining carbon element and the reaction between the oxygen from the TiO₂ nanoparticles and the incorporated carbon element using an Al Kα X-ray source in an UHV system with a chamber base pressure of ~10⁻¹⁰ Torr.

Optical absorption was used to analyze the absorption peak of the resultant dye solutions after dye adsorption on the porous TiO₂ films to determine the amount of dye adsorbed on the surface. The solutions were placed in cuvettes and were scanned in the analysis chamber from 900 to 400 nm wavelengths. The intensity of the absorption peak of the resultant dye solution was compared to that of the absorption peak of the initial N719 dye solution with a concentration of ~5×10⁻⁴ M in ethanol to determine the amount of moles adsorbed.

The electrochemical experiments were obtained using a conventional three-electrode cell connected to a CHI instruments 660B source unit and 500 W xenon light source that was focused to give 100 mW cm⁻² (the equivalent of one sun at AM 1.5 at the surface of the test cell).

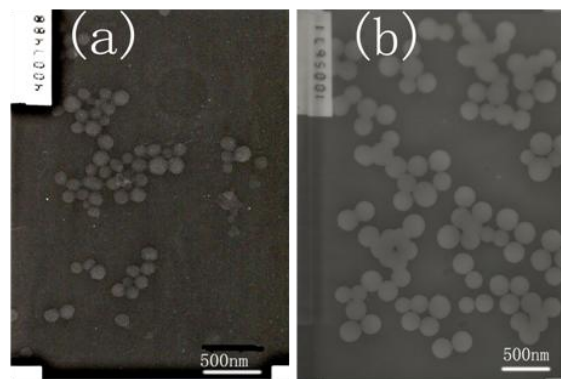


Figure 1. TEM micrographs of carbon spheres (a) with the diameters of 100 nm and (b) with the diameters of 200 nm.

RESULTS AND DISCUSSION

Figure 1 shows the TEM images of carbon spheres. It can be seen that the prepared carbon spheres are regular and smooth, with the average particle sizes of 100 and 200 nm.

SEM analysis was used to examine morphology of the films. Figure 2 shows that the three-dimensional continuous high porosity of the TiO₂ films was formed. Comparing Figure 2 (b) and (c), (d) and (e), respectively, it was found that the more the carbon spheres were incorporated, the larger the average sizes of the particles and the pores increased. Comparing Figure 2 (b) and (d), (c) and (e), it was also found that the TiO₂ electrode modified by 100 nm carbon spheres had smaller particles and more dense structure than that modified by 200 nm carbon spheres. Therefore, the sample modified by 1 wt% carbon spheres with the diameter of 100 nm had the smallest particles and the most dense structure compared with the bare TiO₂ electrode and other samples. Consequently, the sample modified by 1 wt% carbon spheres of 100 nm should have the largest surface area and the greatest number of contact points between sintered colloidal particles or at the interface between the particles and the underlying substrate, which allows the most dye adsorption. These results depended greatly on reactions between the carbon spheres and oxygen partially from the TiO₂ lattices and partially from air atmosphere to form CO₂ gas in the high-temperature sintering process. The difference in the short-circuit photocurrent might be caused between the modified TiO₂ film by 1 wt% carbon spheres with bigger diameters and that by 1 wt% carbon spheres with smaller diameters due to their surface area (that is the amount of dye adsorbed). Support for this anticipation is given below.

Figure 3 shows the XRD spectra of the modified TiO₂ electrodes by the carbon spheres with the different weight ratios and diameters. The results of the XRD measurements demonstrated that there was no change in the position of the peak corresponding to the main (1 0 1)

plane of anatase phase. It was found that the (1 0 1), (2 0 0), (2 1 1), (0 0 4) and (1 1 4) peaks were present for all the films, representing the anatase, the (1 1 0) and (1 0 5) peaks for the rutile phase due to the use of P25 powder (Degussa). Furthermore, the appearance of (1 1 6) peak for the rutile phase implied that the particle size was increased owing to the high-temperature annealing.

The particle sizes of each TiO₂ film samples shown in Table 1 were estimated at each peak using the Scherrer's equation:

$$D = \frac{K\lambda}{B \cos \theta} \quad (4)$$

where K is the Scherrer constant; D is grain size (nm), B is half points width, θ is diffraction angle, λ is X-ray wavelength. Table 1 summarized the effect of the incorporated carbon spheres with different diameters on the properties of the nanoporous TiO₂ electrodes. According to the data, the particle size is changed in a certain extent, irrespective of the size of carbon spheres incorporated in the TiO₂ paste. However, the grain size of the TiO₂ particles increased with the amount of carbon spheres and this may be correlated with the phase transformation of few TiO₂ nanoparticles from anatase to rutile (Gregg, 2004). Furthermore, the specific surface area of the electrode increased when the size of carbon spheres was smaller. The TiO₂ electrode containing 1 wt% of carbon spheres with smaller size showed the higher specific surface area than that containing 1 wt% of carbon spheres with 200 nm diameters and the control sample. And it also presented the highest specific surface area in the all samples.

In order to prove whether carbon spheres were completely oxidized in the annealing process and explain why the surface area of the sample was raised, an XPS analysis was recorded. The remaining carbon element in the TiO₂ films modified by 2, 3 wt% carbon spheres annealed for 30 min in the second step was demonstrated by the XPS analysis (not shown here), which induced the charge recombination, the decreased fill factor and the lower conversion efficiency. So these samples were annealed for 50 min in the second step to remove the carbon element completely. Figure 4(1) shows the XPS variation of the Ti 2p core level peaks for the control sample TiO₂ film (a) and containing 1 wt% of carbon spheres with the diameters of 100 nm (b) before annealing. The peak position of pure TiO₂ is known to be 458.5 eV. The Ti 2p core peak (a) of the TiO₂ samples accords with the standard data without any movement (as that of the other samples incorporated by the carbon spheres with different diameters and amount). And Figure 4(2) shows the XPS spectrum of the annealed control sample (a') and the TiO₂ film containing 1 wt% of carbon spheres with the diameters of 100 nm (b') at 550 °C for 30 min in the second process. In the chart, the Ti 2p core level (b') is strongly asymmetric and an obvious shoulder

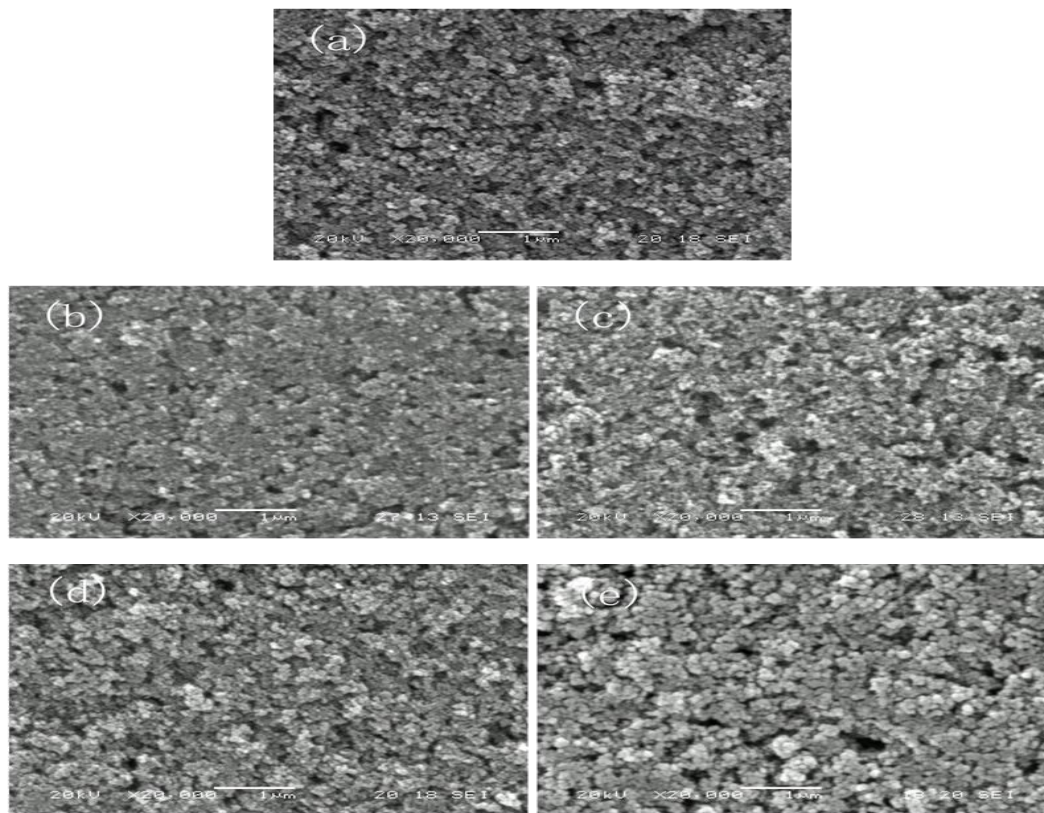


Figure 2. SEM micrographs of (a) the TiO_2 control sample, the modified TiO_2 electrode by (b) 1 wt% and (c) 3 wt% carbon spheres with the diameters of 100 nm and the modified TiO_2 electrode by (d) 1 wt% and (e) 3 wt% carbon spheres with the diameters of 200 nm after sintering at high temperature.

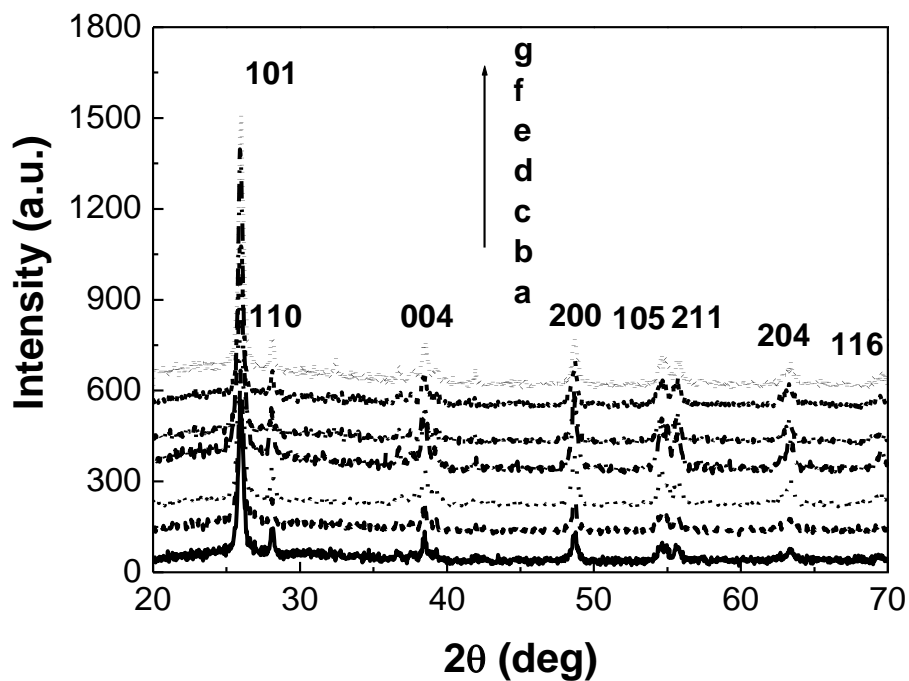


Figure 3. XRD pattern of the annealed films for (a) the control sample, modified by (b) 1 wt%, (c) 2 wt%, (d) 3 wt% carbon spheres with the diameters 100 nm and modified by (e) 1 wt%, (f) 2 wt%, (g) 3 wt% carbon spheres with the diameters 200 nm.

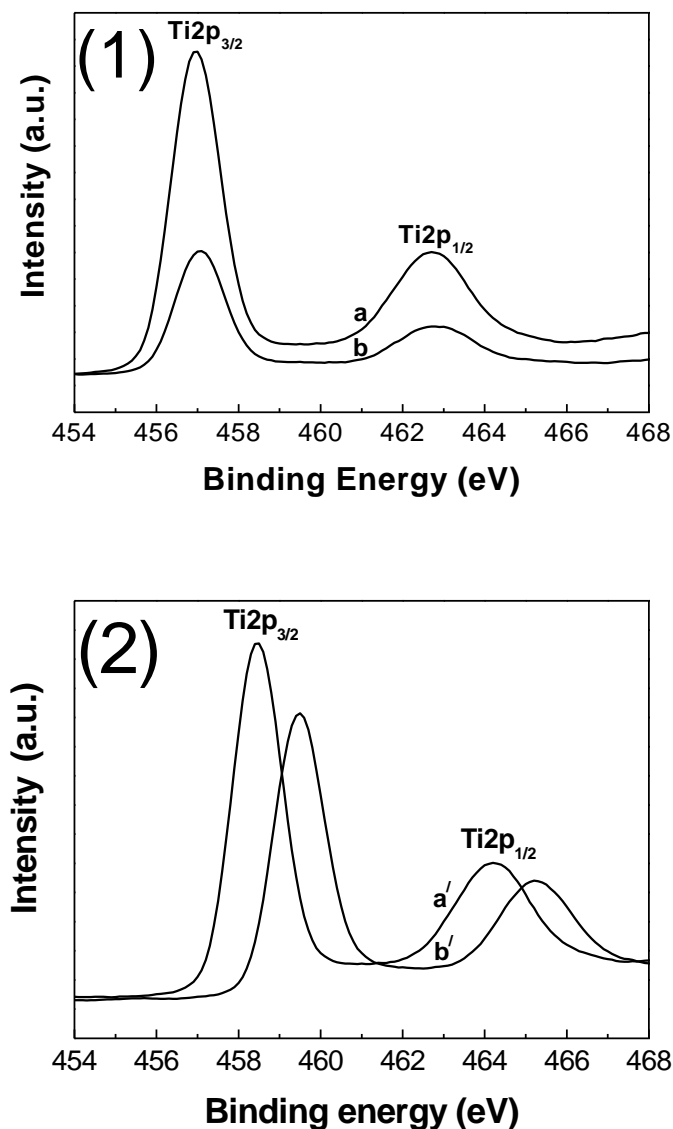


Figure 4. XPS of the samples. (1) the Ti 2p core level peak for (a) the control sample and (b) the modified TiO₂ electrode (1 wt% carbon spheres with the diameters of 100 nm insertion). (2) the Ti 2p core level peak for (a') the control sample and (b') the modified TiO₂ electrode (1 wt% carbon spheres with the diameters of 100 nm) after removing the incorporated carbon spheres by sintering at high temperature (550 °C).

is on the binding energy side (465.1 and 459.5 eV) of the main peak, which strongly proves the chemical reactions between the oxygen from the TiO₂ lattices and the incorporated carbon spheres. So for the TiO₂ film containing 1 wt% of carbon spheres, the chemical valence of the Ti ions was reduced from Ti⁴⁺ to Ti^{X+} (where X = 3.96, 3.9, ...) (Zhang et al., 2003) (as that of the other samples with the carbon spheres being completely oxidized).

The amount of the dye adsorption comparison is the TiO₂ transparent thin films effectively and greatly increased

the absorption of the TiO₂ electrodes in the visible light range, the distinct in the amount of the adsorbed dye, which correlates with the estimated difference in surface area, was evident. Moreover, the modified TiO₂ film with 1 wt% carbon spheres with the diameters of 100 nm, which might be in favor of absorbing light and the diffusion coefficients of electrons so as to improve the solar cell performance, displayed stronger absorption in comparison with all the other sensitized TiO₂ films. The higher capability of the TiO₂ anode modified with 1 wt% of carbon spheres to adsorb more dyes can be ascribed to the higher surface area.

Table 1 summarizes the measured and calculated values obtained from the I-V curves of each solar cell. Figure 5 shows the typical current–voltage characteristics of the cells fabricated using unmodified TiO₂ electrode and the modified TiO₂ electrodes by the 1 wt% of carbon spheres with the diameters of 100 and 200 nm, respectively. These experiment data shown were repeatedly conducted three times and were successfully obtained. According to the data in Table 1, the TiO₂ electrodes modified by 1 wt% carbon spheres with different diameters showed better performance as compared to the control sample. Because the incorporated carbon spheres increase the amount of the pore, the surface area and the roughness of the semiconductor surface so that a large number of dye molecules can be adsorbed directly to the surface and can simultaneously be in direct contact with the redox electrolyte (O'Regan et al., 1991). At the same time, the resulted larger surface areas increase the surface states, which act on the trapping and detrapping sites of photoelectrons or become a pathway for electron transfer in the electrode/electrolyte interface, inducing the charge recombination (Kang et al., 2007b).

The cell fabricated using the TiO₂ electrodes modified with more carbon spheres (2, 3 wt%) with the same diameters showed lower efficiency and lower fill factor contrasting with the control sample and the samples containing less carbon spheres. The efficiency was reduced due to the less absorption of the dye caused by the decreased surface area and the lower photocurrent for the longer calcinations under air ambient (the samples annealed for 50 min) in the second step. The decreased fill factor resulted from the resistance of the cell, the sum of the sheet resistances of the conducting glass substrate (FTO) and counter electrode and the resistance of the substrate-TiO₂ owing to be annealed for a longer time in the second step.

The cell fabricated using the TiO₂ electrode modified by 1 wt% of carbon spheres with the diameters of 100 nm showed the best performance. In this case, a V_{oc} value of 0.71V, a J_{sc} value of 12.00 mA cm⁻², a fill factor (f.f.) of 56.92%, and an efficiency of 4.85% were obtained. Although the voltage of open circuit was smaller, these results in general were better than those of the control presented in Table 1. Though the dye was adsorbed onto

Table 1. Effects of the incorporated carbon spheres with different diameters and amounts on the performance of the dye-sensitized solar cell.

	Particle size (nm)	BET (m^2g^{-1})	Dye adsorption (mmol kg^{-1})	Voc (V)	Jsc (mA cm^{-2})	Fill factor (f.f)	Efficiency (%)
C 0 wt%	30.4	50.68	30.70	0.72	9.29	54.12	3.62
C 100 nm							
C 1 wt%	26.5	67.54	53.42	0.71	12.00	56.92	4.85
C 2 wt%	27.7	55.26	26.93	0.69	9.06	53.27	3.33
C 3 wt%	28.8	56.37	28.40	0.70	9.32	53.80	3.51
C 200 nm							
C 1 wt%	28.3	59.24	47.95	0.72	10.52	55.05	4.17
C 2 wt%	29.5	48.40	27.12	0.69	9.06	53.75	3.36
C 3 wt%	32.1	52.15	28.73	0.70	9.58	53.09	3.56

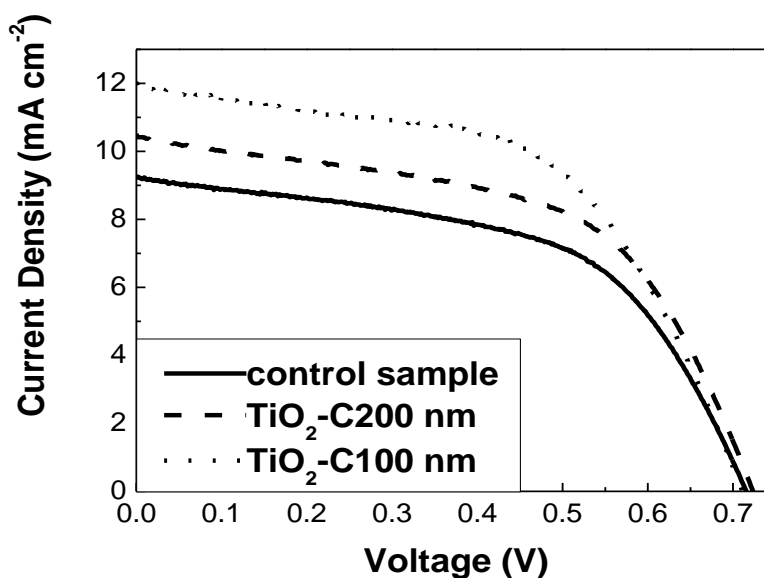


Figure 5. Photovoltaic characteristics of the dye-sensitized solar cell based on 1 wt% carbon spheres with the diameters of 100 nm and 200 nm incorporated TiO_2 electrodes and control sample.

sample (V_{oc} : 0.72V, J_{sc} : 9.29 mA cm^{-2} , fill factor (f.f.): 54.12%, efficiency: 3.62%) and the incorporated TiO_2 electrode by the 1 wt% carbon spheres with the diameters of 200 nm (V_{oc} : 0.72V, J_{sc} : 10.52 mA cm^{-2} , fill factor (f.f.): 55.05%, efficiency: 4.17%). The most notable trend was the change in current of short circuit density and photoelectric conversion efficiency. The changes were relevant to the smaller particles, a larger surface area and a greater number of contact points between sintered particles or at the interface between the particles and the underlying substrate, allowing for greater dye adsorption so as to be in direct contact with the redox electrolyte (Ni et al., 2006). And these attributed to the decrease in the electron loss at the electron transfer in the interface of TiO_2 electrode/electrolyte (Sharma et al.,

2010). Furthermore, comparing with the nanoparticles, the incorporated TiO_2 electrode by the 1 wt% carbon spheres with the diameters of 100 nm provide a faster electron transfer rate due to a decreased number of contact barriers between particles (Yu et al., 2010). All these factors contribute to the improvement of photovoltaic conversion performance of TiO_2 DSSCs.

Conclusion

In conclusion, carbon spheres were prepared with diameters ranging from 100 to 200 nm and used as a new kind of porosity-inducing material. Thermal treatment at high sintering temperature (550°C) plays an

important role in eliminating carbon elements incorporated in the samples by causing reaction between the oxygen from the TiO₂ lattice and the carbon spheres to form CO₂ gas. The introduction of carbon spheres influences the specific surface area and porosity of the nanoparticulated TiO₂ film. Different amounts and sizes of carbon spheres have different effects. Especially, the TiO₂ electrode modified with 1 wt% carbon spheres with the diameter of 100 nm showed excellent performances: a V_{oc} of 0.71 V, a J_{sc} of 12.00 mA cm⁻², a fill factor of 56.92% and an efficiency of 4.85%. Experimental results confirm the possibility of fabricating dye-sensitized solar cells using nanometer-sized carbon spheres. Consequently, a new approach is suggested for further detailed studies on the improvement of the performance of DSSCs by using nanometer-sized carbon spheres.

ACKNOWLEDGMENTS

The authors acknowledge The Science and Technology Department and The Education Department of Henan Province of China for research funds (Nos 082300460070, 2008A140001).

REFERENCES

- Benkstein KD, Kopidakis N, Lagemaat JVD, Frank AJ (2003). Influence of the percolation network geometry on electron transport in dye-sensitized titanium dioxide solar cells. *J. Phys. Chem., B* 107: 7759-7767.
- Chou TP, Zhang QF, Russo B, Fryxell GE, Cao GZ (2007). Titania particle size effect on the overall performance of dye-sensitized solar cells. *J. Phys. Chem., C* 111: 6296-6302.
- Fang X, Ma T, Guan G, Kida T, Abe E (2004). Effect of Pt film thickness of a counter electrode on the performance of dye-sensitized solar cell. *J. Electroanal. Chem.*, 570: 257-263.
- Grätzel M (2004). Conversion of sunlight to electric power by nanocrystalline dye-sensitized solar cells. *J. Photochem. Photobiol. A. Chem.*, 164: 3-14.
- Grätzel M (2007). Photovoltaic and photoelectrochemical conversion of solar energy. *Phil. Trans. R. Soc., A* 365: 993-1005.
- Gregg BA (2004). Interfacial processes in the dye-sensitized solar cell. *Coord. Chem. Rev.*, 248: 1215-1224.
- Hara K, Nishikawa T, Kurashige M, Kawauchi H, Kashima T, Sayama K, Aika K, Arakawa H (2005). Influence of electrolyte on the photovoltaic performance of a dye-sensitized TiO₂ solar cell based on a Ru(II) terpyridyl complex photosensitizer. *Sol. Energy Mater. Sol. Cells*, 85: 21-30.
- Kang SH, Kim JY, Kim YK, Sung YE (2007a). Effects of the incorporation of carbon powder into nanostructured TiO₂ film for dye-sensitized solar cell. *J. Photochem. Photobiol. A. Chem.*, 186: 234-241.
- Kang SH, Kim JY, Sung YE (2007b). Role of surface state on the electron flow in modified TiO₂ film incorporating carbon powder for a dye-sensitized solar cell. *Electrochim. Acta*, 52: 5242-5250.
- Lagemaat JVD, Benkstein KD, Frank AJ (2001). Relation between particle coordination number and porosity in nanoparticle films: Implications to dye-sensitized solar cells. *J. Phys. Chem., B* 105: 12433-12436.
- Lee KM, Suryanarayanan V, Ho KC (2009). Influences of different TiO₂ morphologies and solvents on the photovoltaic performance of dye-sensitized solar cells. *J. Power. Sourc.*, 188: 635-641.
- Mor GK, Shankar K, Paulose M, Varghese OK, Grimes CA (2006). Use of highly-ordered TiO₂ nanotube arrays in dye-sensitized solar cells. *Nano Lett.*, 6: 215-218.
- Nakade S, Saito Y, Kubo W, Kitamura T, Wada Y, Yanagida S (2003). Influence of TiO₂ nanoparticle size on electron diffusion and recombination in dye-sensitized TiO₂ solar cells. *J. Phys. Chem., B* 107: 8607-8611.
- Nazeeruddin MK, Pechy P, Renouard T, Zakeeruddin SM, Baker RH, Comte P, Liska P, Cevey L, Costa E, Shklover V, Spiccia L, Deacon GB, Bignozzi CA, Grätzel M (2001). Engineering of efficient panchromatic sensitizers for nanocrystalline TiO₂-based solar cells. *J. Am. Chem. Soc.*, 123: 1613-1624.
- O'Regan B, Grätzel M (1991). A low-cost high-efficiency solar-cell based on dye-sensitized colloidal TiO₂ films. *Nature*, 353: 737-740.
- Park NG, Lagemaat JVD, Frank AJ (2000). Comparison of dye-sensitized rutile- and anatase-based TiO₂ solar cells. *J. Phys. Chem., B* 104: 8989-8994.
- Podraza NJ, Chen C, Sainju D, Ezekoye O, Horn MW, Wronski CR, Collins RW (2005). Transparent conducting oxide sculptured thin films for photovoltaics applications. *Mater. Res. Soc. Symp. Proc.*, 865: 273-278.
- Saito Y, Kambe S, Kitamura T, Wada Y, Yanagida S (2004). Morphology control of mesoporous TiO₂ nanocrystalline films for performance of dye-sensitized solar cells. *Sol. Energy Mater. Sol. Cells*, 83: 1-13.
- Sharma GD, Suresh P, Roy MS, Mikroyannidis JA (2010). Effect of surface modification of TiO₂ on the photovoltaic performance of the quasi solid state dye sensitized solar cells using a benzothiadiazole-based dye. *J. Power. Sourc.*, 195: 3011-3016.
- Shen Q, Toyoda T (2003). Studies of optical absorption and electron transport in nanocrystalline TiO₂ electrodes. *Thin Solid Films*, 438-439: 167-170.
- Song MY, Kim DK, Ihn KJ, Jo SM, Kim DY (2004). Electrospun TiO₂ electrodes for dye-sensitized solar cells. *Nanotechnology*, 15: 1861-1865.
- Sun X, Li Y (2004). Colloidal carbon spheres and their core/shell structures with noble-metal nanoparticles. *Angew. Chem., Int. Ed. Engl.*, 43: 597-601.
- Tan B, Wu YY (2006). Dye-sensitized solar cells based on anatase TiO₂ nanoparticle/nanowire composites. *J. Phys. Chem., B* 110: 15932-15938.
- Tao RH, Wu JM, Xue HX, Song XM, Pan X, Fang XQ, Fang XD, Dai SY (2010). A novel approach to titania nanowire arrays as photoanodes of back-illuminated dye-sensitized solar cells. *J. Power Sourc.*, 195: 2989-2995.
- Wang H, Liu Y, Xu HM, Dong X, Shen H, Wang YH, Yang HX (2009). An investigation on the novel structure of dye-sensitized solar cell with integrated photoanode. *Renew. Energ.*, 34: 1635-1638.
- Wang ZS, Kawauchi H, Kashima T, Arakawa H (2004). Significant influence of TiO₂ photoelectrode morphology on the energy conversion efficiency of N719 dye-sensitized solar cell. *Coord. Chem. Rev.*, 248: 1381-1389.
- Yu JG, Fan JJ, Zhao L (2010). Dye-sensitized solar cells based on hollow anatase TiO₂ spheres prepared by self-transformation method. *Electrochimica. Acta*, 55: 597-602.
- Zhang M, Wang XD, Wang FM, Li WH (2003). Oxygen sensitivity of nano-CeO₂ coating TiO₂ materials. *Sens. Actuators, B* 92:167-170.
- Zhao D, Peng TY, Lu LL, Cai P, Jiang P, Bian ZQ (2008). Effect of annealing temperature on the photoelectrochemical properties of DSSCs made with m-TiO₂ nanoparticles. *J. Phys. Chem., C*, 112: 8486-8494.